Brain infection by wild-type SARS-CoV-2 and the B.1.617.2 and B.1.1.529 variants of concern is a severe outcome in K18-hACE2 transgenic mice

Yicheng He [1*#], Jill Henley[2*], Philip Sell[1,2*] and Lucio Comai[1,2#]

[1]Department of Molecular Microbiology and Immunology, [2]Hastings Foundation and Wright Foundation BSL3 laboratory, Keck School of Medicine, University of Southern California, Los Angeles, CA 90089

*: equal contributions

#: corresponding authors (heyichen@usc.edu; comai@usc.edu)

Abstract

Background: SARS-CoV-2 is a respiratory virus with neurological complications including loss of smell and taste, headache, and confusion that can persist for months or longer. Severe neuronal cell damage has also been reported in some cases. The objective of this study was to compare the infectivity of Wild-type, Delta, and Omicron variants in transgenic mice that express the human angiotensin-converting enzyme 2 (hACE2) receptor under the control of the keratin 18 promoter (K18) and characterize the progression of infection and inflammatory response in the lung and brain of these animals.

Methods: K18-hACE2 female mice were intranasally infected with Wild-type, Delta, or Omicron variants and euthanized either at 3 days post-infection (dpi) or at the humane endpoint. None of the animals infected with the Omicron variant reached the humane endpoint and were euthanized at day 8 dpi. Virological and immunological analyses were performed in the lungs, olfactory bulbs, medulla oblongata, and brains.

Results: We established that Wild-type, Delta, and Omicron infect the lung and brain of K18-hACE2 mice. At 3 dpi, mice infected with the Omicron variant show lower levels of viral RNA than those infected with Wild-type or Delta in the lung and brain. However, they still demonstrate upregulation of cytokines and chemokines, indicating that the Omicron variant can induce pulmonary and neuronal inflammation despite reduced viral proliferation after infection. At the humane endpoint/8dpi, there is a significant increase in viral RNA in mice infected with the Wild-type or Delta variant brains. However, viral RNA levels in Omicron-infected mice did not increase significantly as compared to 3dpi, and the expression of cytokines and chemokines in the brain, olfactory bulb, and medulla oblongata was downregulated, suggesting that infection by the Omicron variant results in attenuated neuroinflammation as compared with Wild-type and Delta.

Introduction

COVID is an infectious disease caused by the severe acute respiratory syndrome coronavirus 2 (SARS-CoV-2) that has affected millions of individuals worldwide. SARS-CoV-2 is a β-coronavirus with a positive-sense RNA genome very similar to SARS-CoV-1 (80%), but more infectious and transmissive due to a higher reproductive number (R0)[1]. SARS-CoV-2 contains five viral proteins, with nucleocapsid (N) protein coating and packaging for RNA genome, membrane (M) protein incorporating viral components into new virions, envelope (E) protein for viral assembly, and spike (S) protein participating in viral entry into host cells[2]. The early mutation found in SARS-CoV-2 is the Spike protein D614G mutation, which is also carried by many SARS-CoV-2 variants including Delta (B.1.617.2) and Omicron (B.1.1.529)[3]. D614G mutation is found to be more efficient in entering the host cell and has increased viral replication in lung

epithelial cells and the upper respiratory tract[4]. However, the D614G mutation doesn't change the S protein affinity to ACE2 or its resistance to antibody neutralization[5].

The Delta (B.1.617.2) variant has several spike protein mutations responsible for its increased infectivity and a higher virion-releasing advantage over other SARS-CoV-2[6]. As Delta S protein is found to be cleaved more predominately than other SARS-CoV-2 variants, it can cause cell membrane fusion, and cell-to-cell syncytia, and infects target cells more efficiently[7]. Among all these mutations, the T478K mutation in the receptor-binding domain (RBD) has been highlighted to be associated with higher infectivity[8], and the P681R mutation is responsible for forming large syncytia and facilitating furin-mediated cleavage[9]. The Omicron (B.1.1.529) variant was found to have a large repertoire of mutations in the spike protein. T478K, N501Y, D614G, and Δ69–70 mutations result in an increased Omicron RBD binding affinity for hACE2[10]. The K417N-E484K-N501Y mutations are also thought to induce S protein conformational changes that contribute to immune escape[11]. The L452R mutation in Omicron shows enhanced glycolysis and S protein cleavage[12]. However, the multiple mutations also resulted in the S protein maintaining pre-fusion conformation[13], reducing its viral replication[14] and cell fusion ability in human lung cells[13]. In vivo tests also showed decreased viral load, attenuated inflammation[15], and pathology[16] in the lung. As Omicron shows replication defect in cells expressing TMPRSS2, it is suggested that Omicron might be more dependent on the endocytic pathway for entering host cells[17].

SARS-CoV-2 is a respiratory virus known to cause acute respiratory distress syndrome[18] as well as neurological complications. Patients being hospitalized due to acute infection have reported different neurological symptoms, including agitation, confusion[12], headache, and impaired consciousness[19]. More severe neuron damages observed from post-mortem samples from patients who died of SARS-CoV-2 are hemorrhage with infarction or white matter lesion, venous thrombosis[20,21] or thrombotic ischemic infarction[21,22] ischemic necrosis[23], edema[24], perivascular or microvascular congestion and injury[23], and hypoxia changes[25,26,27]. Cerebrospinal fluid (CSF) in patients who showed neurological diseases have elevated cytokine levels, indicating neurological inflammation even though no SARS-CoV-2 RNA was detected by qPCR[28]. However, SARS-CoV-2 can cross the blood-brain barrier and induce neuroinflammation[29]. Infection of human neural progenitor cells shows enhanced expression of viral transcription and metabolic processes, highlighting the ability of SARS-CoV-2 to hijack the host neuron cells to replicate[30]. SARS-CoV-2 can also infect non-neuronal cells, inducing upregulation of genes related to pro-inflammatory response and endoplasmic reticulum (ER)[31]. It has also been reported that the S1 subunit of the S protein can cross the blood-brain barrier[32] and activate microglial cells to increase cytokine release and inflammasome activities[33,34]. Here, we examined viral infection caused by Wild-type, Delta, and Omicron in the lung and brain of the well-characterized k18 hACE2 transgenic mouse model.

Methods

Mice and viruses

All animal procedures were performed at the ABSL3 facility of Keck School of Medicine at the University of Southern California and approved by the Institutional Animal Care and Use Committee (IACUC) and the Institutional Biosafety Committee (IBC) of the University of Southern California.

K18 hACE2 transgenic mice were obtained from the Jackson laboratory (strain #: 034860). Mice of different ages and both sexes were intranasally inoculated with SARS-CoV-2 and variants at 10^4 PFU and euthanized at the humane endpoint or 8 dpi.

The wild-type SARS-CoV-2, the Delta and Omicron SARS-CoV-2 variants of concern were obtained from the BEI repository (Wild-type (USA-WA1/2020, catalog: NR-52281), Delta (B.1.617.2, catalog: NR-55671), and Omicron (B.1.1.529, catalog: NR-56461) and propagated and tittered in Vero-E6 cells. Work with SARS-CoV-2 was performed in a biosafety level 3 laboratory.

Measurement of viral burden

Total RNA was collected from infected mouse tissues at the indicated time points using TRIzol reagent (Thermo Fisher Scientific) according to the manufacturer's instructions. Complementary DNA (cDNA) was synthesized from DNase-treated RNA using iScript Reverse Transcription Supermix for RT-qPCR (BIO-RAD catalog: 1708841). RNA samples were normalized to 100ng/µl. 10µl volume reaction was used with 2µl of iScript RT Supermix and 1µl RNA template input (100ng). Reaction protocol for cDNA synthesis: priming 5 min at 25°C, reverse transcription 20min at 46°C, RT inactivation 1min at 95°C. Copies of the SARS-CoV-2 nucleocapsid (N1) gene were determined using IDT Primetime Gene Expression Master mix (Cat#1055770). 2019-nCoV_N1 primer was obtained from IDT (Cat#10007007). The primer sequence of N1 gene: Forward Primer: 5'-GAC CCC AAA ATC AGC GAA AT-3' Reverse Primer: 5'-TCT GGT TAC TGC CAG TTG AAT CTG-3' Probe: 5'-FAM-ACC CCG CAT TAC GTT TGG TGG ACC BHQ1-3'. ActB control was ordered from IDT (Mm.PT. 39a.22214843.g Cat# 1077852).10µl volume reaction was used with 5µl Primetime Gene Expression Master mix(2x), 1µl cDNA template, 0.75µl for N1 primer probe or 1µl for Act B primer-probe (final reaction concentration: 500nM). Reaction protocol RT-qPCR: Primer melting 15 min at 50°C, DNA denaturing 2 min at 95°C, denaturation 3 sec at 95, annealing 30 sec at 55°C. Standards for SARS-CoV-2 quantification were also run with the same protocol.

Measurement of cytokines and chemokines mRNA

RNA of lung, brain, and brain subregions were extracted using the kit mentioned above. Complementary DNA (cDNA) was synthesized from DNase-treated RNA using iScript Reverse Transcription Supermix for RT-qPCR (BIO-RAD catalog: 1708841). 20µl volume reaction was used with 4ul of iScript RT Supermix and 2µl RNA template input (normalized to 100ug/µl). Reaction protocol for cDNA synthesis: priming 5 min at 25°C, reverse transcription 20min at 46°C, RT inactivation 1min at 95°C. Cytokine and chemokine expression were determined using SsoAdvanced Universal SYBR Green Supermix (BIO-RAD catalog: 1725271). 10 µl volume reaction was used with 5 µl SsoAdvanced Universal SYBR Green Supermix(2x), 1 µl cDNA template, and 0.5 µl each forward and reverse primer (final reaction concentration: 500nM). Reaction protocol RT-qPCR (SYBR Green): Initial DNA denature 30 sec at 95°C, denature 15 sec at 95°C,

annealing/extension 30 sec at 60°C (40 cycles). Melt Curve was run after the completion of qPCR. Primer sets are:

CXCL9(F: CCTAGTGATAAGGAATGCACGATG, R: CTAGGCAGGTTTGATCTCCGTTC); CXCL10 (F: ATCATCCCTGCGAGCCTATCCT, R: GACCTTTTTTGGCTAAACGCTTTC); CCL8 (F: GGGTGCTGAAAAGCTACGAGAG, R: GGATCTCCATGTACTCACTGACC); VEGF-a (F: GCACTGGACCCTGGCTTTAC, R: ATCGGACGGCAGTAGCTTCG), CCL2(F: TGTTCACAGTTGCCGGCTG, R: GCACAGACCTCTCTCTTGAGC); IFN-γ (F: CAGCAACAGCAAGGCGAAAAAGG, R: TTTCCGCTTCCTGAGGCTGGAT); TNF-α (F: GGTGCCTATGTCTCAGCCTCTT, R: GCCATAGAACTGATGAGAGGGAG); CXCL11(F: CCGAGTAACGGCTGCGACAAAG, R: CCTGCATTATGAGGCGAGCTTG); IL-6(F: ACCCCAATTTCCAATGCTCTCCT, R: ACGCACTAGGTTTGCCGAGTA); IL-1β (F: TGGACCTTCCAGGATGAGGACA, R: GTTCATCTCGGAGCCTGTAGTG); IL-10 (F: CGGGAAGACAATAACTGCACCC, R: CGGTTAGCAGTATGTTGTCCAGC); GM-CSF (F: CCTGGGCATTGTGGTCTACAG, R: GGCATGTCATCCAGGAGGTT); G-CSF (F: GCAGACACAGTGCCTAAGCCA, R: CATCCAGCTGAAGCAAGTCCA)

Results

Disease progression of SARS-CoV-2 infection of k18 hACE2 mice

K18-ACE2 transgenic mice were infected with 10^4 PFU of either Wild-type, Delta (B.1.617.2) or Omicron (B.1.1.529) SARS-CoV-2 and their weight and health conditions were recorded over a period of 7 to 8 days. Mice infected with the Wild-type virus started to show weight loss at 6dpi and reached the humane endpoint between 6dpi and 7dpi (Figure 1). Disease progression was slightly faster in mice infected with the Delta variant, which started to lose weight at 4 dpi and reached the humane endpoint as early as 5 dpi. Weight loss and moderate to severe neurological signs (head tilting, poor ambulation) were the prominent criteria for the humane endpoint in mice infected with the Wild-type or Delta SARS-CoV-2. In contrast, mice infected with the Omicron variant did not display any weight loss past 8 dpi and invariably survived the infection with no sign of neurological symptoms.

Pulmonary inflammation and infection of K18 hACE2 mice

Based on the differences in clinical manifestations between mice infected with the Wild-type, Delta, or Omicron SARS-CoV-2, we compared the viral load and inflammation in the lung at 3dpi and humane endpoint. Mice infected with the Omicron variant were euthanized at day 8dpi to make a meaningful comparison with the mice infected with Wild-type or Delta. At 3dpi, the lungs of mice infected by the Wild-type or Delta SARS-CoV-2 show comparable viral loads, while mice infected with Omicron have significantly lower levels of viral RNA (Figure 2a). Notably, infection by the Delta variant induced significantly higher levels of chemokine mRNAs such as CXCL9, CXCL10, CXCL11, and CCL2 than Wild-type. There is minimal induction of cytokines and chemokines RNA detected in mice infected with the Omicron SARS-CoV-2 at 3dpi. (Figure 2c). At the humane endpoint, there is a significantly higher amount of viral RNA in the lungs of mice infected with the Delta variant than Wild-type, while viral RNA in mice infected with Omicron remains relatively low. (Figure 2b). Nevertheless, mice infected with Omicron display a similarly high level of mRNAs for inflammatory cytokines and chemokines as compared

to the Wild-type or Delta virus (Figure 2d). Thus, despite the lower levels of viral RNA, pulmonary inflammation is not attenuated in mice infected with Omicron.

Infection and inflammation in the brain of k18 hACE2 mice

Next, we compared brain infection and neuroinflammation by SARS-CoV-2 variants. As observed in the lungs, a high level of viral infection in the Delta variant was observed in the brains of infected mice at 3 dpi. Viral RNA presents in low amounts in the brains of mice infected with the Wild-type. Interestingly, the brains of mice infected with Omicron display significantly higher levels of viral RNA than mice infected with Wild-type viruses (Figure 3a). The brains of mice infected with the Omicron variant showed high mRNA levels of the inflammatory cytokines and chemokines tested in the experiment, while mice infected with the Delta variant showed increased levels only for a subset of them despite the higher amount of viral RNA in their brain. (Figure 3c). At the humane endpoint, viral RNA levels were high in mice infected with Wild-type or Delta (Figure 3b). Mice infected with either the Wild-type or the Delta variant also showed a significant upregulation of inflammatory markers. In contrast, mice infected with the Omicron variant showed low levels of viral RNA and downregulation of inflammatory markers at 8 dpi. (Figure 3b, 3d).

Infection and inflammation in the medulla oblongata (MO) of k18 hACE2 mice

The medulla oblongata is a possible route for SARS-CoV-2 infection of the brain. At 3 dpi, the medulla oblongata of mice infected with the Delta variant displayed more viral RNA than mice infected with either the Wild-type or Omicron (Figure 4a). However, infection by any of these SARS-CoV-2 viruses resulted in mild upregulation of inflammatory markers such as IL-1β, TNF-α, and IL-10 (Figure 4c). At the humane endpoint, we detected a significant increase in viral RNA in the medulla oblongata of mice infected with the Wild-type or the Delta variant. A less severe increase in viral RNA levels was observed in the medulla oblongata of mice infected with the Omicron variant. (Figure 4b) At the humane endpoint, inflammatory markers were significantly upregulated in mice infected with Wild-type or Delta but downregulated in mice infected with the Omicron variant. (Figure 4 d).

Infection and inflammation in the olfactory bulb (OB) of k18 hACE2 mice

The loss of smell observed in SARS-CoV-2 infected individuals suggests that the olfactory bulb may be the route for SARS-CoV-2 invasion into the brain. We examined the levels of viral RNA and inflammatory response in the olfactory bulb of mice infected with Wild-type, Delta, and Omicron SARS-CoV-2 at the human endpoint (Wild-type and Delta) or 8dpi (omicron) and observed a pattern similar to that seen in the medulla oblongata. The olfactory bulb of mice infected with the Wild-type or Delta variant shows high levels of viral RNA and inflammatory markers. Mice infected with Omicron show low levels of viral RNA and decreased expression of the inflammatory markers as compared to uninfected controls (Figure 5a,5b).

Discussion

The neurological impact of SARS-CoV-2 has been debated since the start of the COVID-19 pandemic. Studies on the relationship between viral loads and neurological inflammation, as well as the impact of different SARS-CoV-2 on the nervous system, have been limited. Here we compared the infectivity by Wild-type, Delta, and Omicron SARS-CoV-2 in transgenic K18-hACE2 mice and characterized the progression of infection and inflammatory response in the lung and brain of these animals. We observed that transgenic mice infected with Omicron display minimal weight loss and reduced disease progression as compared to mice infected with the Wild-type and Delta variant, which is in line with the viral infection studies in hamsters [35,36,37]. Mice infected with the Delta variant have higher viral RNA levels and increased expression of inflammatory markers levels at the humane endpoint in the lung, suggesting that this SARS-CoV-2 variant results in enhanced lung infection and cellular damage. The high levels of lung inflammation caused by the Delta variant were also observed in other studies using k18 hACE2 mice[38,39]. Interestingly, although viral RNA levels in the lung of Omicron-infected mice are significantly lower, infection by this variant induced a high level of inflammation at both 3dpi and 8dpi as compared to Wild-type and Delta. As the upregulation of proinflammatory cytokines has been reported to be related to reduced lung function and tissue damage in both acute and post-acute infections,[40,41,42] the high expression level of inflammatory genes we found in lungs of mice infected by either Wild-type, Delta, or Omicron is likely to be causing lung tissue damage and reduced lung function in post-acute infections.

Our analysis of the brain of mice infected with the Omicron variant shows reduced viral RNA levels as compared to the brain of mice infected with Wild-type or Delta at 3dpi and humane endpoint/8dpi. These results were also observed in a double humanized mouse model infected with these viruses[43]. The brain of mice infected with Omicron shows downregulation of inflammatory markers at 8dpi suggesting that infection by this variant results in attenuated neurological consequences as compared with mice infected with either Wild-type or Delta. This outcome is in agreement with the reported lack of neurological symptoms after the Omicron outbreak in human cohort studies[44,45].

In the olfactory bulb of mice infected with the Omicron variant, we detected low levels of viral RNA at 8dpi as compared to Delta and Omicron at the human endpoint, which is in line with the low viral load of the Omicron variant observed in the olfactory bulb in infected hamsters.[46] Also, mice infected with Wild-type or Delta still induced high levels of inflammation while the Omicron variant showed downregulation of cytokines, suggesting a milder impact of Omicron in olfactory cell function. This result is in line with cohort studies that reported reduced loss of smell and taste in many patients infected with the Omicron variant[47,48]. We detected viral RNA and inflammation in the medulla oblongata of mice infected with Wild-type, Delta, or Omicron. This is consistent with the detection of the virus and activation of immune response cells in the brainstems of COVID-19 patients[49]. However, the inflammatory response in this region of the brain was mild in mice infected with the Omicron variant.

Collectively, these data demonstrate that K19-hACE2 mice infected with Wild-type, Delta, or Omicron display viral RNA and inflammatory response in the lung as well as brain, olfactory bulb, and medulla oblongata. However, the inflammatory response in the brain, olfactory bulb, and medulla oblongata of mice infected by the Omicron variant is generally milder and does not lead to health conditions that require euthanasia.

Reference

1. Cevik M, Kuppalli K, Kindrachuk J, Peiris M. Virology, transmission, and pathogenesis of SARS-CoV-2. BMJ. 2020;371:m3862. Published 2020 Oct 23. doi:10.1136/BMJ.m3862
2. Hartenian, Ella, et al. "The molecular virology of coronaviruses." The Journal of Biological Chemistry vol. 295,37 (2020): 12910-12934. doi:10.1074/jbc.REV120.013930
3. Arora P, Sidarovich A, Krüger N, et al. B.1.617.2 enters and fuses lung cells with increased efficiency and evades antibodies induced by infection and vaccination. Cell Rep. 2021;37(2):109825. doi:10.1016/j.celrep.2021.109825
4. Plante, Jessica A et al. "Spike mutation D614G alters SARS-CoV-2 fitness." Nature vol. 592,7852 (2021): 116-121. doi:10.1038/s41586-020-2895-3
5. Zhang, L., Jackson, C.B., Mou, H. et al. SARS-CoV-2 spike-protein D614G mutation increases virion spike density and infectivity. Nat Commun 11, 6013 (2020). https://doi.org/10.1038/s41467-020-19808-4
6. Mlcochova P, Kemp SA, Dhar MS, et al. SARS-CoV-2 B.1.617.2 Delta variant replication and immune evasion. Nature. 2021;599(7883):114-119. doi:10.1038/s41586-021-03944-y
7. Zhang J, Xiao T, Cai Y, et al. Membrane fusion and immune evasion by the spike protein of SARS-CoV-2 Delta variant. Science. 2021;374(6573):1353-1360. doi:10.1126/science.abl9463
8. Jhun H, Park HY, Hisham Y, Song CS, Kim S. SARS-CoV-2 Delta (B.1.617.2) Variant: A Unique T478K Mutation in Receptor Binding Motif (RBM) of Spike Gene. Immune Netw. 2021;21(5):e32. Published 2021 Oct 11. doi:10.4110/in.2021.21.e32
9. Saito A, Irie T, Suzuki R, et al. Enhanced fusogenicity and pathogenicity of SARS-CoV-2 Delta P681R mutation. Nature. 2022;602(7896):300-306. doi:10.1038/s41586-021-04266-9
10. Lupala CS, Ye Y, Chen H, Su XD, Liu H. Mutations on RBD of SARS-CoV-2 Omicron variant result in stronger binding to human ACE2 receptor. Biochem Biophys Res Commun. 2022;590:34-41. doi:10.1016/j.bbrc.2021.12.079
11. Tian D, Sun Y, Xu H, Ye Q. The emergence and epidemic characteristics of the highly mutated SARS-CoV-2 Omicron variant [published online ahead of print, 2022 Feb 3]. J Med Virol. 2022;10.1002/jmv.27643. doi:10.1002/jmv.27643
12. Helms J, Kremer S, Merdji H, Clere-Jehl R, Schenck M, Kummerlen C, Collange O, Boulay C, Fafi-Kremer S, Ohana M, Anheim M, Meziani F. Neurologic Features in Severe SARS-CoV-2 Infection. N Engl J Med. 2020 Jun 4;382(23):2268-2270. DOI: 10.1056/NEJMc2008597
13. Hui KPY, Ho JCW, Cheung MC, et al. SARS-CoV-2 Omicron variant replication in the human bronchus and lung ex vivo. Nature. 2022;603(7902):715-720. doi:10.1038/s41586-022-04479-6
14. Cui Z, Liu P, Wang N, et al. Structural and functional characterizations of infectivity and immune evasion of SARS-CoV-2 Omicron. Cell. 2022;185(5):860-871.e13. doi:10.1016/j.cell.2022.01.019
15. Halfmann PJ, Iida S, Iwatsuki-Horimoto K, et al. SARS-CoV-2 Omicron virus causes attenuated disease in mice and hamsters. Nature. 2022;603(7902):687-692. doi:10.1038/s41586-022-04441-6
16. Shuai H, Chan JF, Hu B, et al. Attenuated replication and pathogenicity of SARS-CoV-2 B.1.1.529 Omicron. Nature. 2022;603(7902):693-699. doi:10.1038/s41586-022-04442-5
17. Zhang Y, Zhang T, Fang Y, Liu J, Ye Q, Ding L. SARS-CoV-2 spike L452R mutation increases Omicron variant fusogenicity and infectivity as well as host glycolysis. Signal Transduct Target Ther. 2022;7(1):76. Published 2022 Mar 9. doi:10.1038/s41392-022-00941-z
18. Di Wu, Tiantian Wu, Qun Liu, Zhicong Yang, The SARS-CoV-2 outbreak: What we know, International Journal of Infectious Diseases, Volume 94, 2020, Pages 44-48, ISSN 1201-9712, https://doi.org/10.1016/j.ijid.2020.03.004.

19. Maury A, Lyoubi A, Peiffer-Smadja N, de Broucker T, Meppiel E. Neurological manifestations associated with SARS-CoV-2 and other coronaviruses: A narrative review for clinicians. Rev Neurol (Paris). 2021;177(1-2):51-64. doi:10.1016/j.neurol.2020.10.001
20. Reichard, R Ross, et al. "Neuropathology of COVID-19: a spectrum of vascular and acute disseminated encephalomyelitis (ADEM)-like pathology." Acta neuropathologic vol. 140,1 (2020): 1-6. doi:10.1007/s00401-020-02166-2
21. Younger, David S. "Postmortem neuropathology in COVID-19." Brain pathology (Zurich, Switzerland) vol. 31,2 (2021): 385-386. doi:10.1111/bpa.12915
22. Wichmann, Dominic, et al. "Autopsy Findings and Venous Thromboembolism in Patients With COVID-19: A Prospective Cohort Study." Annals of Internal Medicine vol. 173,4 (2020): 268-277. doi:10.7326/M20-2003
23. Remmelink M, De Mendonça R, D'Haene N, et al. Unspecific post-mortem findings despite multiorgan viral spread in COVID-19 patients. Crit Care. 2020;24(1):495. Published 2020 Aug 12. doi:10.1186/s13054-020-03218-5
24. Fabbri VP, Foschini MP, Lazzarotto T, et al. Brain ischemic injury in COVID-19-infected patients: a series of 10 post-mortem cases. Brain Pathol. 2021;31(1):205-210. doi:10.1111/bpa.12901
25. Schurink B, Roos E, Radonic T, et al. Viral presence and immunopathology in patients with lethal COVID-19: a prospective autopsy cohort study. Lancet Microbe. 2020;1(7):e290-e299. doi:10.1016/S2666-5247(20)30144-0
26. von Weyhern CH, Kaufmann I, Neff F, Kremer M. Early evidence of pronounced brain involvement in fatal COVID-19 outcomes. Lancet. 2020;395(10241):e109. doi:10.1016/S0140-6736(20)31282-4
27. Lee MH, Perl DP, Nair G, et al. Microvascular Injury in the Brains of Patients with Covid-19. N Engl J Med. 2021;384(5):481-483. doi:10.1056/NEJMc2033369
28. Espíndola OM, Gomes YCP, Brandão CO, et al. Inflammatory Cytokine Patterns Associated with Neurological Diseases in Coronavirus Disease 2019. Ann Neurol. 2021;89(5):1041-1045. doi:10.1002/ana.26041
29. Krasemann S, Haferkamp U, Pfefferle S, et al. The blood-brain barrier is dysregulated in COVID-19 and serves as a CNS entry route for SARS-CoV-2. Stem Cell Reports. 2022;17(2):307-320. doi:10.1016/j.stemcr.2021.12.011
30. Song E, Zhang C, Israelow B, et al. Neuroinvasion of SARS-CoV-2 in human and mouse brain. J Exp Med. 2021;218(3):e20202135. doi:10.1084/jem.20202135
31. Gi Uk Jeong, Jaemyun Lyu, Kyun-Do Kim, Young Cheul Chung, Gun Young Yoon, Sumin Lee, Insu Hwang, Won-Ho Shin, Junsu Ko, June-Yong Lee, View ORCID ProfileYoung-Chan Kwon. "SARS-CoV-2 Infection of Microglia Elicits Pro-inflammatory Activation and Apoptotic Cell Death" doi: https://doi.org/10.1101/2022.01.04.475015
32. Rhea EM, Logsdon AF, Hansen KM, et al. The S1 protein of SARS-CoV-2 crosses the blood-brain barrier in mice. Nat Neurosci. 2021;24(3):368-378. doi:10.1038/s41593-020-00771-8
33. Frank MG, Nguyen KH, Ball JB, et al. SARS-CoV-2 spike S1 subunit induces neuroinflammatory, microglial and behavioral sickness responses: Evidence of PAMP-like properties. Brain Behav Immun. 2022;100:267-277. doi:10.1016/j.bbi.2021.12.007
34. Olajide OA, Iwuanyanwu VU, Adegbola OD, Al-Hindawi AA. SARS-CoV-2 Spike Glycoprotein S1 Induces Neuroinflammation in BV-2 Microglia. Mol Neurobiol. 2022;59(1):445-458. doi:10.1007/s12035-021-02593-6
35. Halfmann, P.J., Iida, S., Iwatsuki-Horimoto, K. et al. SARS-CoV-2 Omicron virus causes attenuated disease in mice and hamsters. Nature 603, 687–692 (2022). https://doi.org/10.1038/s41586-022-04441-6

36. McMahan K, Giffin V, Tostanoski LH, et al. Reduced pathogenicity of the SARS-CoV-2 omicron variant in hamsters. Med. 2022;3(4):262-268.e4. doi:10.1016/j.medj.2022.03.004
37. Armando, F., Beythien, G., Kaiser, F.K. et al. SARS-CoV-2 Omicron variant causes mild pathology in the upper and lower respiratory tract of hamsters. Nat Commun 13, 3519 (2022). https://doi.org/10.1038/s41467-022-31200-y
38. Lee KS, Wong TY, Russ BP, Horspool AM, Miller OA, Rader NA, Givi JP, Winters MT, Wong ZYA, Cyphert HA, Denvir J, Stoilov P, Barbier M, Roan NR, Amin MS, Martinez I, Bevere JR, Damron FH. SARS-CoV-2 Delta variant induces enhanced pathology and inflammatory responses in K18-hACE2 mice. PLoS One. 2022 Aug 29;17(8):e0273430. doi: 10.1371/journal.pone.0273430. PMID: 36037222; PMCID: PMC9423646.
39. Víctor J. Costela-Ruiz, Rebeca Illescas-Montes, Jose M. Puerta-Puerta, Concepción Ruiz, Lucia Melguizo-Rodríguez, SARS-CoV-2 infection: The role of cytokines in COVID-19 disease, Cytokine & Growth Factor Reviews, Volume 54, 2020, Pages 62-75, ISSN 1359-6101, https://doi.org/10.1016/j.cytogfr.2020.06.001.
40. Shea A. Lowery, Alan Sariol, Stanley Perlman, Innate immune and inflammatory responses to SARS-CoV-2: Implications for COVID-19, Cell Host & Microbe, Volume 29, Issue 7, 2021, Pages 1052-1062, ISSN 1931-3128,https://doi.org/10.1016/j.chom.2021.05.004.
41. Trinkmann F, Müller M, Reif A, Kahn N, Kreuter M, Trudzinski F, Eichinger M, Heussel CP, Herth FJF; Lung Network Rhine-Neckar-Region. Residual symptoms and lower lung function in patients recovering from SARS-CoV-2 infection. Eur Respir J. 2021 Feb 25;57(2):2003002. doi: 10.1183/13993003.03002-2020. PMID: 33479105; PMCID: PMC7821834.
42. Littlefield KM, Watson RO, Schneider JM, Neff CP, Yamada E, Zhang M, Campbell TB, Falta MT, Jolley SE, Fontenot AP, Palmer BE. SARS-CoV-2-specific T cells associated with inflammation and reduced lung function in pulmonary post-acute sequelae of SARS-CoV-2. PLoS Pathog. 2022 May 26;18(5):e1010359. doi: 10.1371/journal.ppat.1010359. PMID: 35617421; PMCID: PMC9176759.
43. Alves RPDS, Wang YT, Mikulski Z, McArdle S, Shafee N, Valentine KM, Miller R, Verma SK, Batiz FAS, Maule E, Nguyen MN, Timis J, Mann C, Zandonatti M, Alarcon S, Rowe J, Kronenberg M, Weiskopf D, Sette A, Hastie K, Saphire EO, Festin S, Kim K, Shresta S. SARS-CoV-2 Omicron (B.1.1.529) shows minimal neurotropism in a double-humanized mouse model. Antiviral Res. 2023 Apr;212:105580. doi: 10.1016/j.antiviral.2023.105580. Epub 2023 Mar 20. PMID: 36940916; PMCID: PMC10027296.
44. Magnusson K, Kristoffersen DT, Dell'Isola A, Kiadaliri A, Turkiewicz A, Runhaar J, Bierma-Zeinstra S, Englund M, Magnus PM, Kinge JM. Post-covid medical complaints following infection with SARS-CoV-2 Omicron vs Delta variants. Nat Commun. 2022 Nov 30;13(1):7363. doi: 10.1038/s41467-022-35240-2. PMID: 36450749; PMCID: PMC9709355.
45. Woo MS, Mayer C, Brehm TT, Andersen G, Weigel A, Löwe B, Lohse AW, Addo MM, Gerloff C, Knobloch JKM, Schulze Zur Wiesch J, Friese MA. Absence of self-reported neuropsychiatric and somatic symptoms after Omicron variant SARS-CoV-2 breakthrough infections. Brain Commun. 2023 Mar 25;5(2):fcad092. doi: 10.1093/braincomms/fcad092. PMID: 37038497; PMCID: PMC10082557.
46. Bauer L, Rissmann M, Benavides FFW, Leijten L, van Run P, Begeman L, Veldhuis Kroeze EJB, Lendemeijer B, Smeenk H, de Vrij FMS, Kushner SA, Koopmans MPG, Rockx B, van Riel D. In vitro and in vivo differences in neurovirulence between D614G, Delta And Omicron BA.1 SARS-CoV-2 variants. Acta Neuropathol Commun. 2022 Sep 5;10(1):124. doi: 10.1186/s40478-022-01426-4. PMID: 36058935; PMCID: PMC9441226.

47. Piersiala K, Kakabas L, Bruckova A, Starkhammar M, Cardell LO. Acute odynophagia: A new symptom of COVID-19 during the SARS-CoV-2 Omicron variant wave in Sweden. J Intern Med. 2022 Jul;292(1):154-161. doi: 10.1111/joim.13470. Epub 2022 Mar 6. PMID: 35170099; PMCID: PMC9115132.
48. Vihta KD, Pouwels KB, Peto TE, Pritchard E, House T, Studley R, Rourke E, Cook D, Diamond I, Crook D, Clifton DA, Matthews PC, Stoesser N, Eyre DW, Walker AS; COVID-19 Infection Survey team. Omicron-associated changes in SARS-CoV-2 symptoms in the United Kingdom. Clin Infect Dis. 2022 Aug 3;76(3):e133–41. doi: 10.1093/cid/ciac613. Epub ahead of print. PMID: 35917440; PMCID: PMC9384604.
49. Emmi A, Rizzo S, Barzon L, Sandra M, Carturan E, Sinigaglia A, Riccetti S, Della Barbera M, Boscolo-Berto R, Cocco P, Macchi V, Antonini A, De Gaspari M, Basso C, De Caro R, Porzionato A. Detection of SARS-CoV-2 viral proteins and genomic sequences in human brainstem nuclei. NPJ Parkinsons Dis. 2023 Feb 13;9(1):25. doi: 10.1038/s41531-023-00467-3. PMID: 36781876; PMCID: PMC9924897.

Acknowledgments

This work was performed at the Hastings Foundation and Wright Foundation Biosafety level 3 (BLS3) laboratory of USC and was funded by a research grant from the W.M. Keck Foundation to L.C.

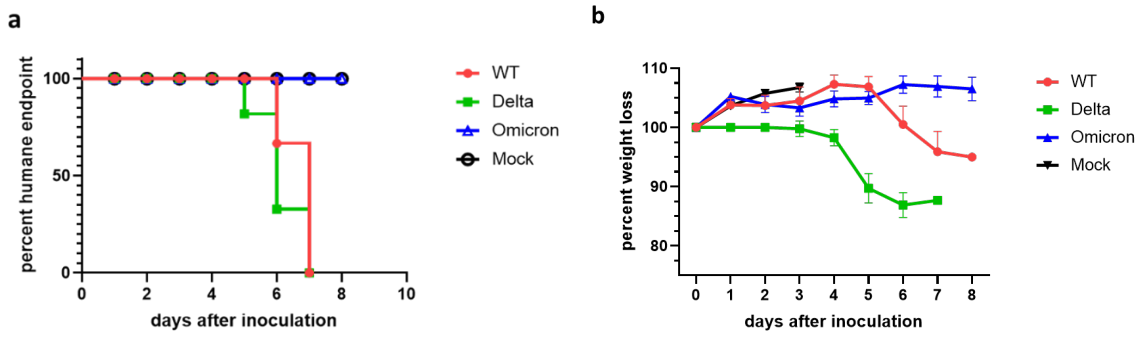

Figure 1. Probability of survival and body weight loss in SARS-CoV-2 infected k18-hACE2 mice. a) Mice were infected at 10^4 PFU, the figure shows the percentage of mice reaching to humane endpoint in days after infection (n=6). Mice infected with Omicron did not reach to humane endpoint but were euthanized at 8 dpi. **b)** Weight loss of uninfected mice(mock) and mice infected with Wild-type, Delta, and Omicron. (n=6) Mean ± s.e.m. Note: uninfected mice weight is only shown over 3 days.

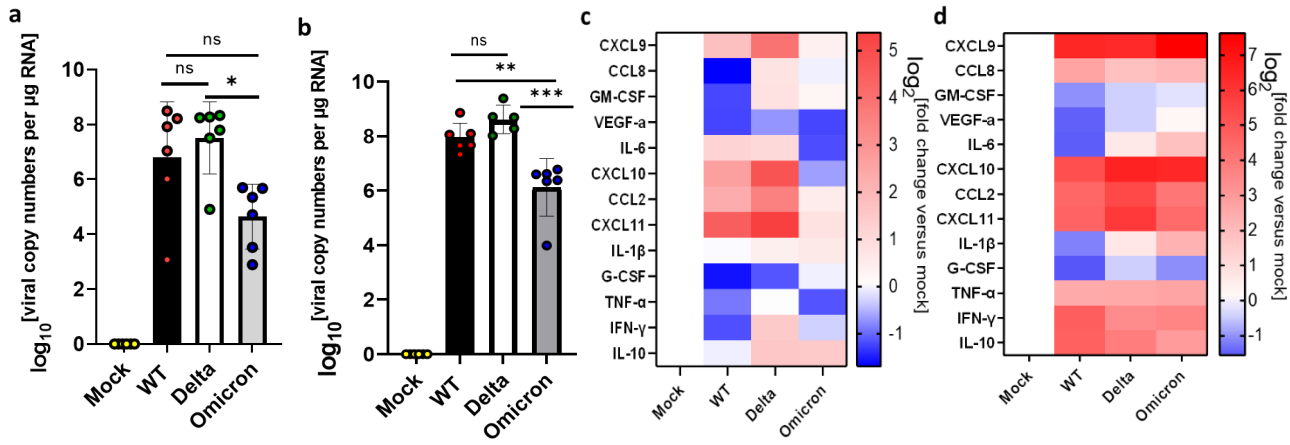

Figure 2. Analysis of viral RNA and cytokines/chemokines in the lungs of SARS-CoV-2 infected K18-hACE2 mice. Mice were infected with SARS-CoV-2 Wild-type, Delta, and Omicron at 10^4 PFU. Mice infected with Delta and Wild-type were euthanized at 3dpi or humane endpoint(5-7dpi). Mice infected with the Omicron variant were euthanized at 3dpi and 8dpi. **a-b**) qPCR of viral copy numbers in the lung at 3 dpi and humane endpoint/8dpi. Mean with SD. One-way ANOVA with Tukey's test was performed *P< 0.05**P< 0.01, ***P< 0.001 **a)** qPCR of SARS-CoV-2 viral copy numbers at 3dpi. Mock (n=4), Wild-type, Delta, and Omicron (n=6) **b)** qPCR of SARS-CoV-2 viral copy numbers at the humane endpoint/8dpi. Wild-type (n=6), Delta (n=5), and Omicron (n=6). **c-d)** Heatmap of cytokines and chemokines levels in the lung. The graph was plotted with Mean. The fold change was calculated using the 2–ΔΔCt method and compared with mock-infected animals. The log2[fold change] was plotted in the corresponding heat map **c)** Heatmap of cytokines and chemokines levels in the lung at 3pi. Mock(n=4), Wild-type (n=6), Delta (n=6), Omicron (n=5). **d)** Heatmap of cytokines and chemokines levels in the lung at the humane endpoint/8dpi. Mock(n=4), Wild-type (n=6), Delta (n=5), Omicron (n=5).

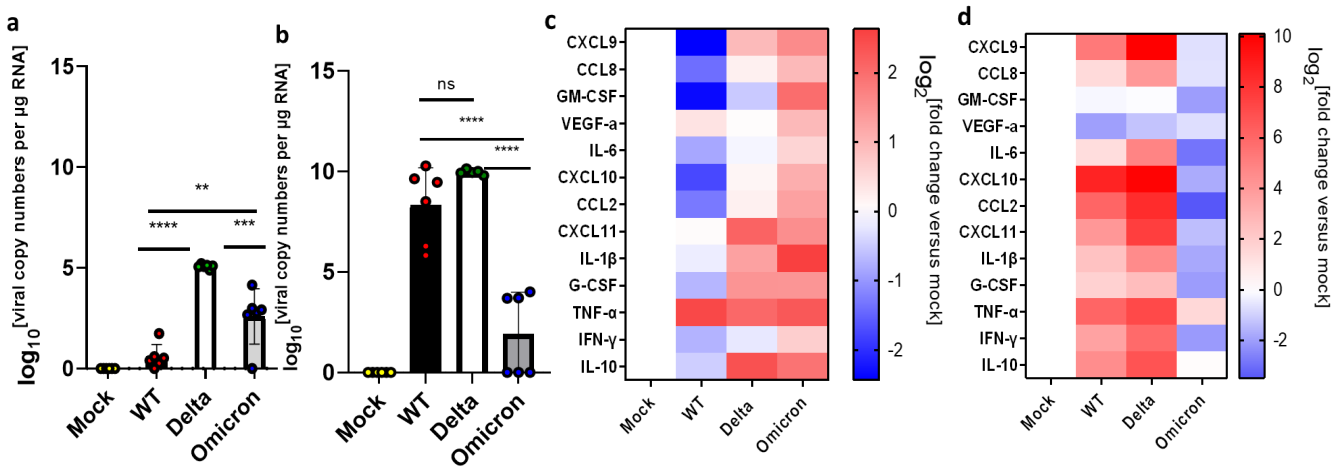

Figure 3. Analysis of viral RNA and cytokines/chemokines in the brain of SARS-CoV-2 infected K18-hACE2 mice. Mice were infected with SARS-CoV-2 Wild-type, Delta, and Omicron at 10^4 PFU. Mice infected with Delta and Wild-type were euthanized at 3dpi and humane endpoint(5-7dpi), and mice infected with the Omicron variant were euthanized at 3dpi and 8dpi. **a-b**) qPCR of viral copy numbers in the brain at 3 dpi (a) and humane endpoint/8dpi (b). Mean with SD. One-way ANOVA with Tukey's test was performed. **p<0.01, ***p<0.001, ****P< 0.0001 **a)** qPCR of SARS-CoV-2 viral copy numbers at 3dpi. Mock (n=4), Wild-type, Delta, and Omicron (n=6) **b)** qPCR of SARS-CoV-2 viral copy numbers at the humane endpoint/8dpi. Mock (n=4), Wild-type (n=6), Delta(n=5) and Omicron (n=6). **c-d)** Heatmap of cytokines and chemokines levels. The graph was plotted with Mean. The fold change was calculated using the 2–ΔΔCt method and compared with mock-infected animals. The log2[fold change] was plotted in the corresponding heat map **c)** Heatmap of cytokines and chemokines levels in the brain at 3pi. Mock(n=4), Wild-type, Delta, and Omicron (n=6). **d)** Heatmap of cytokines and chemokines levels in the brain at the humane endpoint/8dpi. Mock(n=4), Wild-type (n=6), Delta (n=5), Omicron (n=5).

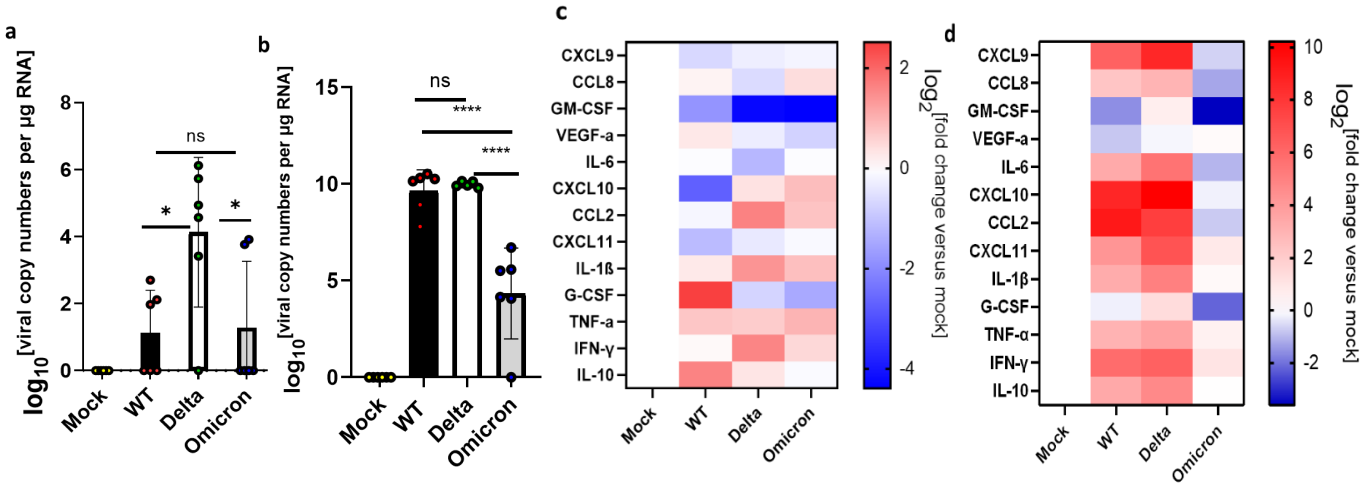

Figure 4. Analysis of viral RNA and inflammatory markers in the medulla oblongata of SARS-CoV-2 infected K18 hACE2 mice. Mice were infected with Wild-type, Delta, and Omicron SARS-CoV-2 at 10^4 PFU. Mice infected with Delta and Wild-type were euthanized 3dpi or at the humane endpoint (5-7 dpi). Mice infected with the Omicron variant were euthanized at 3dpi and 8 dpi. **a)** qPCR of viral copy numbers at 3dpi. Mean with SD. One-way ANOVA with Tukey's test was performed ****P< 0.0001 Mock (n=4), Wild-type (n=6), Delta(n=5) and Omicron (n=6) **b)** qPCR of viral copy numbers at humane endpoint/8dpi. Mean with SD. One-way ANOVA with Tukey's test was performed *P< 0.01 Mock (n=4), Wild-type, Delta, and Omicron (n=6) **c)** Heatmap of cytokines and chemokines levels at 3dpi. Mock (n=4), Wild-type, Delta, and Omicron (n=6). **d)** Heatmap of cytokines and chemokines levels at the humane endpoint/8dpi. The graph was plotted with Mean. The fold change was calculated using the 2–ΔΔCt method and compared with mock-infected animals. The log2[fold change] was plotted in the corresponding heat map. Mock(n=4), Wild-type (n=6), Delta (n=5), Omicron (n=6).

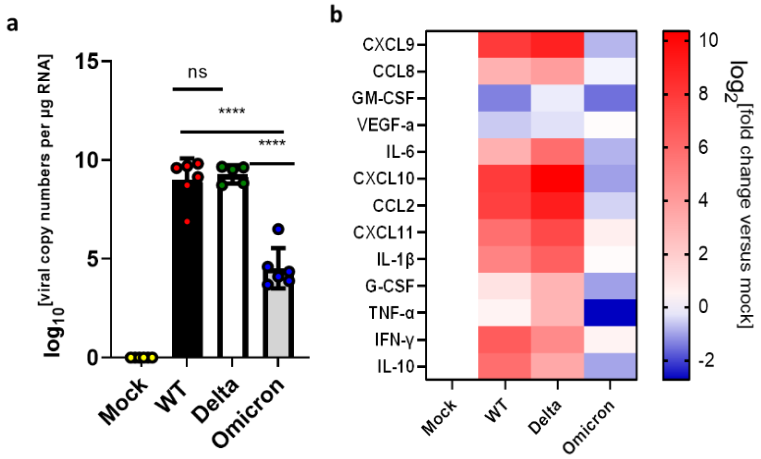

Figure 5. Analysis of viral RNA and inflammatory markers in the olfactory bulb of SARS-CoV-2 k18-hACE2 infected mice. Mice were infected with SARS-CoV-2 wild-type, Delta, or Omicron at 10^4 PFU. Mice infected with Wild-type or Delta were euthanized at the humane endpoint(5-7dpi), while mice infected with the Omicron variant were euthanized at 8dpi. **a)** qPCR of viral copy numbers in the OB at the humane endpoint/8dpi. Mean with SD. One-way ANOVA with Tukey's test was performed ****P< 0.0001 Mock (n=4), Wild-type (n=6), Delta(n=5) and Omicron (n=6) **b)** Heatmap of cytokines and chemokines levels at the humane endpoint/8dpi. The graph was plotted with Mean. The fold change was calculated using the 2–ΔΔCt method and compared with mock-infected animals. The log2[fold change] was plotted in the corresponding heat map. Mock(n=4), Wild-type (n=6), Delta (n=5), Omicron (n=6).